

Assessment of Mitral Regurgitation Severity with Intensity Based Region Growing

M. L. Dewal^{*}, Kalpana Saini^{1*} and Manojkumar Rohit[#]

^{*}*Dept of Electrical Engineering, Indian institute of Technology Roorkee,
Uttarakhand, India, 247667*

[#]*Department of Cardiology, Advanced Cardiac Centre, Post Graduate Institute of
Medical Education & Research, Chandigarh, India, 160012*

Abstract

The color Doppler echocardiography allows the clinician and researchers to identify the blood flow patterns, direction, and velocity in case any dis-functioning like valvular and regurgitation stenosis. Jet area is the most used method by the clinicians for MR severity because it is directly proportional to severity of MR.

Methods

A method is developed for automatic segmentation of jet area and finding the jet area value in numerical terms. Intensity based region growing has been used for segmentation. Before this some preprocessing steps have been applied to make the image suitable for intensity based region growing. Total nine images have been examined taken from the different patients suffering from mitral regurgitation.

Results

Proposed method finds the two cases are under the moderate MR category and other seven detected as the case of severe MR. in case of clinical point of view three cases are to be found under the moderate and six under the category of severe MR.

Conclusions

This work is expected to enhance the clinician's capability in fast determining the extent of severity of mitral regurgitation. The algorithm developed is capable of removing the spurious areas during the process of segmentation.

Keywords: *color Doppler, Regurgitation, Stenosis, Severity, Segmentation*

1. Introduction

Change in color pattern from color passive red or blue to a mosaic pattern indicates heart abnormality. The difference of color in Color Doppler image shows the velocity magnitude and direction of blood flow which is encoded into color patterns. Conventionally, blood cells moving away from the transducer are usually displayed in blue, while blood cells moving towards the transducer are displayed in red and mosaic pattern is formed when there exist mitral regurgitation. The aim has been carryout auto-segmentation of the mosaic pattern and of the colored background and further to correlate MR severity to the area of the MR regurgitant area.

The aim of image segmentation is to divide the jet area from the background image. There are many methods to carryout image segmentation. These methods may be histogram thresholding [1-6], edge based segmentation [7-10], graph based approaches

¹ Corresponding Author:
Kalpana Saini,
e-mail: kal_2312@rediffmail.com
Tel: +919410559865

[11, 12], region growing [13-22], clustering [23-32] probabilistic or Bayesian approaches [33-37] neural networks for segmentation [38].

For accomplishing segmentation of mosaic patterned jet area out of the color background, one needs to carry out a good amount of preprocessing of the color Doppler image, which includes finding out (i) region of interest for getting color portion of the image and (ii) its conversion to gray scale to make it suitable for carrying out intensity based region growing segmentation. Region growing on the basis of intensity difference has been approached to get the MR jet area segmented. The value of the jet area is the dimensional value of the inner object in the segmented jet area. The post processing step has been included to remove the spurious areas around the actual jet area. The method proposed has the advantage of accurately estimating the jet area automatically and thereby save the time of clinicians or provide corroborative estimate with increased accuracy. Focusing and defocusing based techniques have been used for the selection of the Region Of Interest (ROI), and the advanced gray color to gray scale conversion has been applied to get the fine intensity and well contrast image.

2. Jet Area Segmentation Using Intensity Based Region Growing (JASRG)

The entire procedure has been implemented in three stages. The first two stages are related to the jet area segmentation algorithm, and the last stage estimate the size of the area. The jet area segmentation is discussed as follows:

2.1 Pre-Processing Stage

As said before, the pre-processing is done to carve out the object of interest and then convert it to format which is suitable for further processing.

2.1.1 Region of Interest: This stage having two procedures first is Region of interest extraction and second is conversion of Red, Green and Blue (RGB) image to gray scale image. Input color Doppler Echocardiography image with regurgitation is the combination of 2-d image and color Doppler image. Color shows the direction and flow of blood, So that color area is Region Of Interest in this case. This can be obtained by removing the background image. This is possible if we have that image also on which that pseudo color is superimposed. Their difference gives the ROI image, *i.e.*, color image.

ROI region can be detected as explained in [39]. However they use this mixture model in-depth for content based image retrieval, but our main concern is to just find out the main region which is related to mitral regurgitation. Formulation of this model is as below:

$$\begin{aligned}
 f_{ROI}(x) &= f(x|F)p(F) + f(x|DF)p(DF), \\
 &= \sum_{j=1}^2 \frac{\pi_j}{\mu_j} \exp\left(-x/\mu_j\right) U_x.
 \end{aligned} \tag{1}$$

Where $x \geq 0$ denotes a particular contrast level, F and DF correspond to focused and defocused regions, respectively and $f(x|F)$, $f(x|DF)$, $p(F)$ and $p(DF)$ showing their corresponding functions, π_j 's are the mixing proportions ($0 \leq \pi_j \leq 1$), $\sum_{j=1}^2 \pi_j = 1$, and μ_j denotes the mean contrast of the j^{th} class. μ_1 corresponds to the contrast distribution in the focused region so $\mu_1 > \mu_2$

2.1.2 Color to Gray Scale Conversion: Second step is conversion of that color image to gray scale image because region growing used is based on intensity of the image. Obtained image is multi intensity image on gray scale. The effective luminance of a pixel can be calculated as in eq. (2).

$$Y = 0.3R + 0.59G + 0.11B \quad (2)$$

Where R is for red color, G for green, color and B is for blue. Every color as well as color combination has its own intensity. Gray levels represent the interval number of quantization in gray scale image processing. Here the image is 8-bit image. There are 256 gray levels in an 8 bit gray scale image, and the intensity of each pixel can have from 0 to 255, with 0 being black and 255 being white.

Other method we apply is as follows:

Let $f_{ROI} = \{f_{ROI}(x,y)\} = \{R(x,y), G(x,y), B(x,y)\}$ is a color

image, we want to find three transform coefficients α, β , and γ to transform f_{ROI} into a grayscale image $fL_{ROI}(x,y) = \{fL_{ROI}(x,y)\} = \{\alpha R(x,y) + \beta G(x,y) + \gamma B(x,y)\}$, where, (x,y) is the spatial co-ordinate of the pixels. The requirement of fL_{ROI} is to have the maximum variance in order to convey the maximum information. However, only maximizing the variance has no guarantee that fL_{ROI} will be visually pleasing or even visually meaningful. Therefore, extra constraints are necessary in order to produce visually plausible maximum variance grayscale image. It needs to set constraints; which may be as follows: First, the transform should be energy preserving.

We should not apply the image's energy but rather should preserve the energy in the grayscale. This means that $\alpha + \beta + \gamma = 1$; and second, the grayscale image should preserve the brightness of the original image. This is an equally important condition. An image and its negative have the same variance. The problem is, thus, formulated as:

Transform f_{ROI} to fL_{ROI} according to

$$fL_{ROI} = \{fL_{ROI}(x,y)\} = \{\alpha R(x,y) + \beta G(x,y) + \gamma B(x,y)\}, \quad (3)$$

The transform coefficients are found as

$$(\alpha, \beta, \gamma) = \underset{\alpha, \beta, \gamma}{\operatorname{arg\,max}} \left(\operatorname{Var} \left(\{fL_{ROI}(x,y)\} \right) \right) \quad (4)$$

Subject to

$$\alpha + \beta + \gamma = 1 \quad (5)$$

And

$$\sum_{(x,y)} fL_{ROI}(x,y) = \frac{1}{3} \sum_{(x,y)} (R(x,y), G(x,y), B(x,y)) \quad (6)$$

Let the average of the Red, Green and Blue channels be M_R, M_G and M_B , respectively; the mean vector of the image $M = (M_R, M_G, M_B)$; Let $u = (\alpha, \beta, \gamma)$.

Let $R = (R(1,1), R(1,2), \dots, R(M,N))$ be the $M \times N$ dimensional array of the red pixels, Where $M \times N$ is the dimension of the image. We define G and B similarly for the green and blue pixels. The covariance matrix of the color channels is

$$\zeta = \begin{bmatrix} R - M_R \\ G - M_G \\ B - M_B \end{bmatrix} \begin{bmatrix} (R - M_R)^T & (G - M_G)^T & (B - M_B)^T \end{bmatrix} \quad (7)$$

The variance of the transformed grayscale image, $Var(fL_{ROI})$, and the average brightness, $A_b(fL_{ROI})$, are

$$Var(fL_{ROI}) = u\zeta u^T \quad A_b(fL_{ROI}) = Mu^T \quad (8)$$

2.2 Jet area Segmentation

The intensity based region growing technique has been used for carrying out segmentation of the jet area. The following operations have been performed to accomplish the segmentation to get the true regurgitant jet area.

2.2.1 Region Growing: Region growing operation segments the image into different regions. The Regions either expand or contract based on the pixel properties and the properties of the neighborhood pixels. Self assessed region growing method has been used for this purpose [40].

Computation has been done for last iteration grown region R_i , (maximum likelihood estimation) ML estimates for the mean (available from last iteration) and standard deviation $\left(\overline{fL}_{ROI(R_{i-1})}, \sigma_{f_{ROI(R_{i-1})}}\right)$.

For every candidate pixel $x_{c_{i-1}}$ being connected to R_{i-1} , $x_{c_{i-1}} \in R_i$ if

$$fL_{ROI}(x_{c_{i-1}}) \in \left[\overline{fL}_{ROI(R_{i-1})} + k_i \sigma_{f_{ROI(R_{i-1})}} \right] \quad (9)$$

The assessment function $O_i(\overline{fL}_{ROI(R_{i-1})}, \overline{fL}_{ROI(P_i)})$ is derived as equation (11) using the intensity average $\overline{fL}_{ROI(R_i)}$ in R_i and the intensity average $\overline{fL}_{ROI(P_i)}$ in the external perimeter P_i of R_i according to normalization equation $\text{mean } \overline{fL}_{ROI(N)} = \frac{1}{N} \sum_{x_k \in N} fL(x_k)$,

where x is a pixel position and $fL(x)$ is the intensity of pixel at x . N is a neighborhood of radius R around the seed and eq.(10):

$$P_i = \{x_{ci}\} \cap R_i^C \quad (10)$$

$$O_i(\overline{fL}_{ROI(R_i)}, \overline{fL}_{ROI(P_i)}) = \left| \frac{\overline{fL}_{ROI(P_i)} - \overline{fL}_{ROI(R_i)}}{\overline{fL}_{ROI(P_i)} + \overline{fL}_{ROI(R_i)}} \right| \quad (11)$$

If O_{i-1} was a local maximum, when compared to O_{i-2} and O_i (only when $i \geq 2$), then the algorithm stops and the output is R_{i-1} ; otherwise it goes for another iteration.

2.2.2 Removing Spurious Areas: Upon implementation of the above procedures some small areas which are not objects of interest are generated. These areas introduce errors in the calculation of jet area and create complexity in finding regurgitant jet area. So it is important to remove these areas. For removing spurious areas there is a need of a threshold value of some pixels below which these areas are removed and a single object

oriented area obtained in the image. Let P be number of pixels below which area is not acceptable

$$\begin{cases} \text{if } Area > P \text{ then } Area \in D_A \\ \text{if } Area \leq P \text{ then } Area \in S_A \end{cases} \quad \text{and} \quad (12)$$

P is the pixel size of the area. D_A is the desired area and S_A is the spurious area.

2.4 Contour Detection of the Segmented Area

The contour is only drawn to represent the segmented area into within a single line. Enclosed area is the desired jet area. Contour is a curve in two dimensions on which the value of a function $f(x, y)$ is a constant. Based on the minimum and maximum values of the segmented image, the number of contour levels and the values of the contour levels are chosen automatically.

Let ϕ be the desired contour, ϕ_i is inside of the contour and ϕ_o outside of the contour then:

$$D_A \in \phi_i \quad (13)$$

And the boundary of this area is on ϕ .

3. Algorithm Summarization

Input: color Doppler image with pseudo color and without pseudo color.

Output: image: segmented portion of jet area and contour of the jet area.

Value: Jet area in cm^2

Step 1: Extraction of ROI image $f_{ROI}(x, y)$ from input image.

Step 2: Obtain gray image from color image $f_{ROI}(x, y) \rightarrow fL_{ROI}(x, y)$

Step 3: If ; the assessment function $O_i(\overline{fL}_{ROI(R_{i-1})}, \overline{fL}_{ROI(P_i)}) \rightarrow$ local maximum region growing

Stops

Otherwise; go to next iteration

Step 4: If; $Area >$ the specified true value of jet area then $Area \in D_A$ (the desired jet area)

Otherwise; $Area \in S_A$ (spurious area)

End;

4. Results

Total nine cases have been taken for this research work. Views selected for color Doppler Echocardiography are parasternal long axis view and Apical two chamber and four chamber views. Images which are taken here cover all the views. Figure1 shows the color Doppler images with Mitral regurgitation. Whereas Figure 2. having the background images without pseudo colors.

When Region Of Interest (ROI) is extracted then all the background pixels become zero and only color pixels remains as an object as shown in Figure 3.

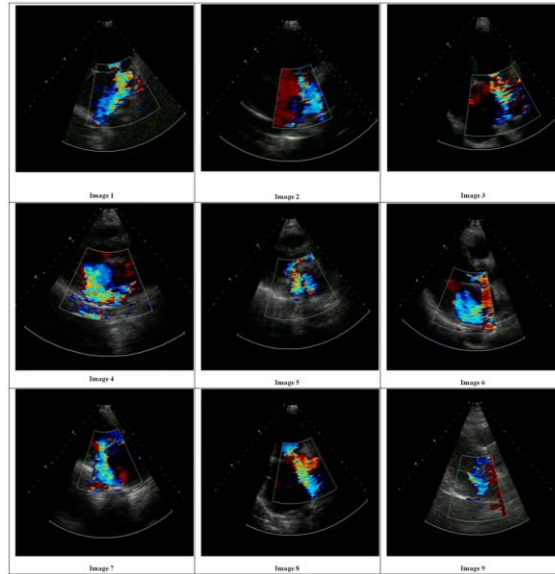


Figure 1. Color Doppler Images with Mitral Regurgitation with Pseudo Color

It can be easily observed in Figure 4 that there are completely blue, completely red and a mosaic pattern of color. Segmentation is required to extract only that area which is covered by mosaic pattern because that is the only area that belongs to the regurgitant jet. Figure 4 shows only the areas of the images that are obtained after applying segmentation and removing spurious areas. Figure 5 shows the contours of these images.

Depending upon the size of the regugitant jet the regurgitation is mild, moderate or severe. In the present work, the MR jet area is determined automatically. Auto-evaluated numerical values of the segmented jet areas and the areas drawn by the clinicians are shown in Table 1. This Table also demonstrates the comparison between these two values; the one obtained by the count of pixels within the auto-segmented jet area, and the other, drawn manually by the clinician.

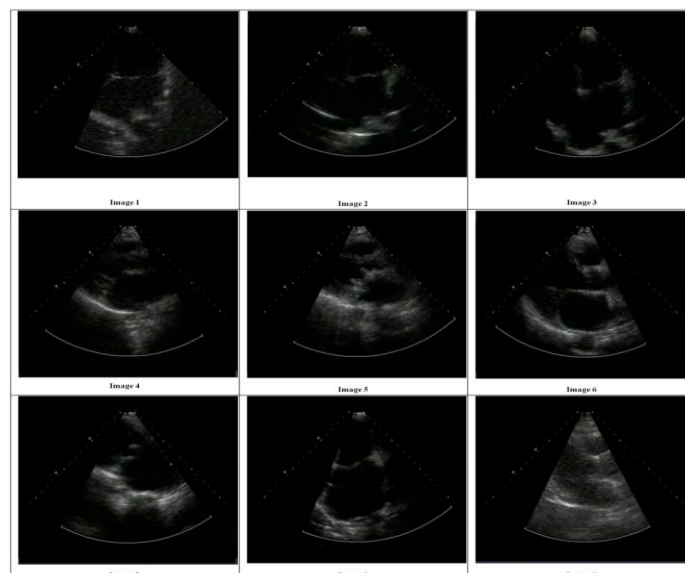


Figure 2. Background Images without Pseudo Color

The work demonstrates the numerical values corresponding to the extent of severity of regurgitation directly in relation to the jet area values of MR obtained through the technique presented in this paper and the values obtained by an expert clinician manually. Values of the MR jet area by clinicians has been taken as ground truth for comparison, because there is no such paper in the literature related to automatic MR jet area detection. From Figure 6 it can be noticed that value of color jet area in both cases *i.e.*, automatic segmentation proposed in this work and the one obtained by clinician are almost the same. There is very less variation in values. There difference is very-very close to zero line except in some values which are also quite near zero line.

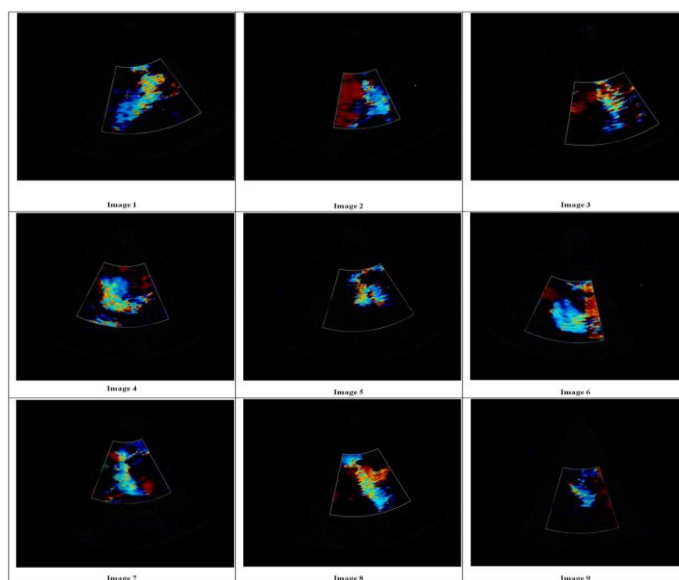


Figure 3. Images with Roi

If the color jet area is less than 4cm^2 then the condition of regurgitation is mild. But if it is up to 10cm^2 then there is moderate regurgitation and if the jet area increases beyond 10cm^2 then it is indication of severe mitral regurgitation. Table 2 shows the patients with mild, moderate and severe mitral regurgitation with proposed algorithm and Table 3 presents the findings carried out by clinician. There is no case of mild regurgitation in both cases. Patients are the same in both the cases. Table 2 shows that proposed method categorized two patients in moderate condition and 7 patients in severe condition. Patients having moderate mitral regurgitation are Patient 3 having jet area 9.43 cm^2 and patient 9 having jet area 6.43 cm^2 . Patients 1, 2, 4, 5, 6, 7, 8 having severe regurgitation having jet area 15.38 cm^2 , 10.92 cm^2 , 13.53 cm^2 , 10.01 cm^2 , 12.98 cm^2 , 11.26 cm^2 , 11.45 cm^2 respectively. Table 3 shows that according to area drawn by clinician three patients 3, 5 and 9 with jet area 9.53 cm^2 , 9.72 cm^2 and 7.57 cm^2 respectively are having moderate mitral regurgitation; whereas the patients 1, 2, 4, 6, 7, and 8 with jet area 15.38 cm^2 , 10.96 cm^2 , 13.61 cm^2 , 12.97 cm^2 , 11.24 cm^2 , 11.35 cm^2 having severe regurgitation.

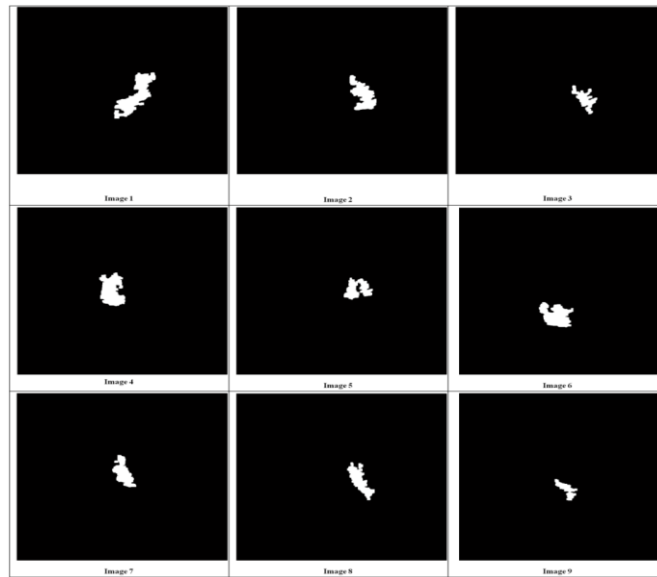


Figure 4. Jet Area Obtained after JASRG

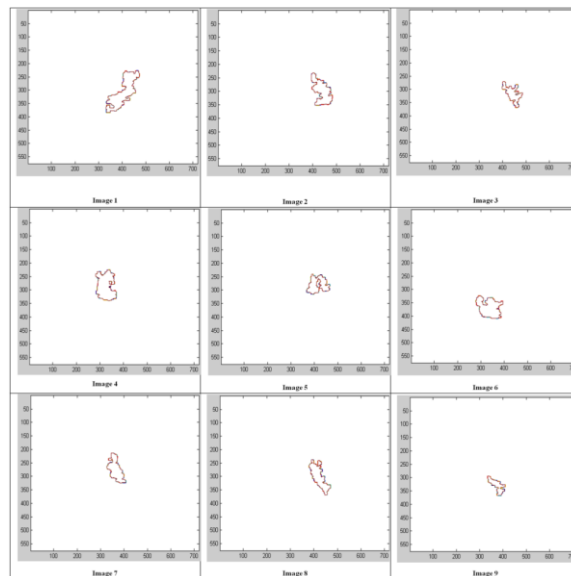


Figure 5. Contours of the Jet Area Showing Boundary

Table 1. Value of Jet Area Obtained from proposed Method (JASRG) and by Clinician

Automatic Jet Area (Pixels)	Automatic Jet Area (Cm ²) A	Jet area drawn by clinician (Cm ²) M	Difference of A-M
8938	15.38	15.39	0.01
4541	10.92	10.86	0.06
3432	9.43	9.38	0.05
7006	13.53	13.23	0.30
4192	10.01	9.72	0.29

6300	12.98	12.94	0.04
4486	11.26	11.29	0.03
4855	11.45	11.86	0.41
2168	6.45	5.59	0.86

Table 2. Severity Grades According Area Drawn by Proposed Automatic Method

Images	Mild	Moderate	Severe
1	–	–	15.38
2	–	–	10.96
3	–	9.43	–
4	–	–	13.61
5	–	–	10.53
6	–	–	12.97
7	–	–	11.24
8	–	–	11.35
9	–	6.43	–

Table 3. Severity Grades According to Area Drawn by Clinician

Images	Mild	Moderate	Severe
1	–	–	15.39
2	–	–	10.86
3	–	9.38	–
4	–	–	13.23
5	–	9.72	–
6	–	–	12.94
7	–	–	11.29
8	–	–	11.86
9	–	5.59	–

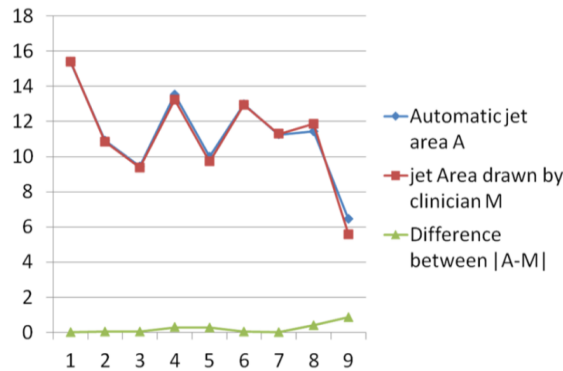


Figure 6. Comparison of Jet Areas Obtained from JASRG and Area Obtained by the Clinicians

5. Conclusions and Discussions

This paper deals with the automatic segmentation of regurgitant jet area and finding its numerical value. So far the clinicians have been drawing the jet area by hand. The important feature of this method, apart from its being automatic, is of this method the speed of processing is very fast. Within a few seconds the desired object is drawn. All the results obtained have been cross-checked with the results obtained by the clinicians and the findings are almost the same within very close limits. Removal of such type of areas is the part of the algorithm. In this paper all cases are of moderate or severe mitral regurgitation.

Funding Information

This research did not receive any specific grant from any funding agency in the public, commercial or not-for-profit sector.

Declaration of Interest

Declare that there is no conflict of interest that could be perceived as prejudicing the impartiality of the research reported.

References

- [1] R. B. Ohlander, "Analysis of natural scenes", PhD Thesis, Carnegie Institute of Technology, Dept. of Computer Science, Carnegie -Mellon University, Pittsburgh, PA, (1975).
- [2] M. Cheriet, J. N. Said, *et al.*, "A recursive thresholding technique for image segmentation", IEEE Transactions on Image Processing, vol. 7, no. 6, (1998), pp. 918-920.
- [3] N. Otsu, "A threshold selection method from grey level histograms", IEEE Transactions on Systems, Man and Cybernetics, vol. 8, (1978), pp. 62-66.
- [4] B. Bhanu and O. D. Faugeras, "Segmentation of images having unimodal distributions", IEEE Transactions on Pattern Recognition and Machine Intelligence, vol. 4, no. 4, (1982), pp. 408-419.
- [5] A. Rosenfeld, "Scene labelling by relaxation operations", IEEE Transactions on Systems, Man and Cybernetics, vol. 6, no. 6, (1976), pp. 420-433.
- [6] N. W. Campbell, W. P. J. B. T. Mackeown, *et al.*, "The automatic classification of outdoor images", Proc. International Conference on Engineering Applications of Neural Networks, Systems Engineering Association, (1996), pp. 339-342.
- [7] N. Ahuja, A. Rosenfeld, *et al.*, "Neighbour gray levels as features in pixel classification", Pattern Recognition, vol. 12, (1980), pp. 251-260.
- [8] I. Y. Kim and H. S. Yang, "Efficient image labelling based on markov random field and error backpropagation network", Pattern Recognition, vol. 26, no. 2, (1995), pp. 1695-1707.
- [9] W. A. Perkins, "Area segmentation of images using edge points", IEEE Transactions on Pattern Recognition and Machine Intelligence, vol. 2, no. 1, (1980), pp. 8-15.
- [10] F. H. Y. Chan, F. K. Lam, *et al.*, "Adaptive thresholding by variational method", IEEE Transactions on Image Processing, vol. 2, no. 3, (1998), pp. 168-174.
- [11] K. Cho and P. Meer, "Image segmentation from consensus information", Computer Vision and Image Understanding, vol. 68, no. 1, (1997), pp. 72-89.
- [12] M. Yeung, B. L. Yeo, *et al.*, "Segmentation of video by clustering and graph analysis, Computer Vision and Image Processing, vol. 71, no. 1, (1998), pp. 94-109.
- [13] N. W. Campbell, B. T. Thomas, *et al.*, "Automatic segmentation and classification of outdoor images using neural networks", International Journal of Neural Systems, vol. 8, no. 1, (1997a), pp. 137-144.
- [14] R. Adams and L. Bischof, "Seeded region growing", IEEE Transactions on Pattern Analysis and Machine Intelligence, vol. 16, no. 6, (1994), pp. 641-647.
- [15] A. Mehnert, P. Jackway, *et al.*, "An improved seeded region growing algorithm", Pattern Recognition Letters, vol. 18, (1997), pp. 1065-1071.
- [16] S. Basu, "Image segmentation by semantic method", Pattern Recognition, (1987), pp. 497-511.
- [17] J. M. Beaulieu and M. Goldberg, "Hierarchy in picture segmentation: a stepwise optimization approach", IEEE Transactions on Pattern Analysis and Machine Intelligence, vol. 11, no. 2, (1989), pp. pp. 150-163.
- [18] J. P. Gambotto, "A new approach to combining region growing and edge detection", Pattern Recognition Letters, vol. 14, (1993), pp. 869-875.

- [19] S. A. Hojjatoleslami and J. Kittler, "Region growing: a new approach", CVSSP Technical Report TR-6/95, University of Surrey, Department of Electronic and Electrical Engineering, (1995).
- [20] N. W. Campbell, W. P. J. Mackeown, *et al.*, "Interpreting image databases by region classification", *Pattern Recognition*, vol. 30, no. 4, (1997b), pp. 555-563.
- [21] H. He and Y. Q. Chen, "Unsupervised texture segmentation using resonance algorithm for natural scenes", *Pattern Recognition Letters*, vol. 21, (2000), pp. 741-757.
- [22] S. Singh and R. Al-Mansoori, "Identification of regions of interest in digital mammograms", *Journal of Intelligent Systems*, vol. 10, no. 2, (2000), pp. 183-217.
- [23] A. K. Jain and R. C. Dubes, "Algorithms for clustering data", Prentice Hall, Englewood Cliffs, N.J, (1998).
- [24] T. Kurita, "An efficient agglomerative clustering algorithm using a heap", *Pattern Recognition*, vol. 24, no. 3, (1991), pp. 205-209.
- [25] H. Frigui and R. Krishnapuram, "A robust competitive clustering algorithm with applications in computer vision", *IEEE Transactions on Pattern Analysis and Machine Intelligence*, vol. 21, no. 5, (1999), pp. 450-465.
- [26] J. Pauwels and G. Frederix, "Finding salient regions in images", *Computer Vision and Image Understanding*, vol. 75, (1999), pp. 73-85.
- [27] J. R. Ohm and P. Ma, "Feature-based cluster segmentation of image sequences", *Proc. IEEE International Conference on Image Processing*, (1997), pp. 178-181.
- [28] M. K. Ng, "A note on constrained k-means algorithm", *Pattern Recognition*, vol. 33, (2000), pp. 515-519.
- [29] R. C. Dubes and A. K. Jain, "Clustering techniques: the user's dilemma", *Pattern Recognition*, vol. 8, (1976), pp. 247-260.
- [30] F. Yarman-Vural and E. Ataman, "Noise, histogram and cluster validity for Gaussianmixture data", *Pattern Recognition*, vol. 20, no. 4, (1985), pp. 385-401.
- [31] R. C. Dubes, "How many clusters are best?-an experiment", *Pattern Recognition*, vol. 20, no. 6, pp. 645-663.
- [32] N. Zahid, M. Limouri, *et al.*, "A new cluster validity for fuzzy clustering", *Pattern Recognition*, vol. 32, (1999), pp. 1089-1097.
- [33] J. F. Haddon and J. F. Boyce, "Image segmentation by unifying region and boundary information", *IEEE Transactions on Pattern Analysis and Machine Intelligence*, vol. 12, no. 10, pp. 929-948.
- [34] J. F. Haddon and J. F. Boyce, "Co-occurrence matrices for image analysis", *Electronics and Communication Engineering Journal*, pp. 71-83.
- [35] J. F. Haddon and J. F. Boyce, "Texture classification of segmented regions of FLIR images using neural networks", *Proc. 1st International Conference on Image Processing*, (1994).
- [36] J. F. Haddon, M. Schneebeli, *et al.*, "Automatic segmentation and classification using a co-occurrence based approach", *Proceedings of Digital Image Technologies II, Techniques and Civil Engineering Applications*, (1997).
- [37] M. L. Comer and E. J. Delp, "Segmentation of textured images using a multi-resolution Gaussian autoregressive model", *IEEE Transactions on Image Processing*, vol. 8, no. 3, (1999), pp. 408-420.
- [38] N. Papamarkos, C. Strouthopoulos, *et al.*, "Multithresholding of colour and graylevel images through a neural network technique", *Image and Vision Computing*, vol. 18, (2000), pp. 213-222.
- [39] C. S. Rajashekhara, "Segmentation and region of interest based image retrieval in low depth of field observations", *Image and Vision computing*, vol. 25, (2007), pp. 1709-1724.
- [40] S. C. Mendoza, B. Acha, C. Serrano, *et al.*, "Self-assessed Contrast-Maximizing Adaptive Region Growing", *Advanced Concepts for Intelligent Vision Systems Lecture Notes in Computer Science*, vol. 5807, (2009), pp. 652-663.

